A Subset of 50 Secretory Granules in Close Contact With L-Type Ca^{2+} Channels Accounts for First-Phase Insulin Secretion in Mouse β-Cells

Sebastian Barg, Lena Eliasson, Erik Renström, and Patrik Rorsman

Capacitance measurements were applied to mouse pancreatic β-cells to elucidate the cellular mechanisms underlying biphasic insulin secretion. We report here that only <50 of the β-cell's >10,000 granules are immediately available for release. The releasable granules tightly associate with the voltage-gated α_{1C} Ca^{2+} channels, and it is proposed that the release of these granules accounts for first-phase insulin secretion. Subsequent replenishment of the releasable pool by priming of previously nonreleasable granules is required for second-phase insulin secretion. The latter reaction depends on intragranular acidification due to the concerted action of granular bafilomycin-sensitive v-type H^+-ATPase and 4,4-diisothiocyanostilbene-2,2-disulfonate–blockable ClC-3 Cl^- channels. Lowering the cytoplasmic ATP/ADP ratio prevents granule acidification, granule priming, and refilling of the releasable pool. The latter finding provides an explanation to the transient nature of insulin secretion elicited by, for example, high extracellular K^+ in the absence of metabolizable fuels.
Diabetes **51 (Suppl. 1):S74–S82, 2002**

A secretory cell typically contains thousands of secretory vesicles/granules. Analysis of the kinetics of exocytosis in a variety of endocrine cells and neurons has led to the proposal that the granules exist in distinct functional pools of granules as illustrated schematically in Fig. 1*A* (1,2). Therefore, only a fraction of the granules/vesicles (<5%) exist in a release-competent state capable of undergoing exocytosis following elevation of the cytoplasmic Ca^{2+} concentration, the readily releasable pool (RRP). A subset of the RRP granules are believed to be situated in the immediate vicinity of the voltage-gated Ca^{2+} channels and are thus rapidly exposed to exocytotic levels of Ca^{2+} during Ca^{2+} channel openings. These granules are released with minimal latency and are therefore referred to as the immediately releasable pool (IRP). Both RRP and IRP granules are connected to the plasma membrane (docked) via trans-SNARE (soluble *N*-ethylmaleimide-sensitive fusion protein [NSF]-attachment protein [SNAP] receptor) complexes. Importantly, the bulk of granules in the cell (>95%) exist in a nonreleasable reserve pool, which must undergo a series of ATP-, Ca^{2+}-, and temperature-dependent reactions to become release-competent (3). These reactions are collectively referred to as priming.

Exocytosis in β-cells exhibits great similarities to the general picture of regulated exocytosis in neurons and other (neuro-)endocrine cells outlined above. Experiments using repetitive stimulation protocols or photorelease of caged Ca^{2+} have indicated that only 50 of the total >10,000 granules (i.e., 0.5%) are immediately available for release (4–6). It is also becoming clear that many of the molecular players involved in neurotransmitter release and in hormone release from neuroendocrine cells (the SNARE proteins) have their counterparts in insulin-secreting β-cells. Accordingly, synaptobrevin, SNAP-25, syntaxin, α-SNAP, NSF, and the putative Ca^{2+}-sensing protein synaptotagmin have been identified in insulin-secreting cells and participate in the release process (reviewed in reference [7]).

Here we consider the evidence for and significance of functional pools of secretory granules in the β-cell. We show that β-cells differ from other endocrine cells characterized to date in that a large fraction of the RRP granules tightly associate with the Ca^{2+} channels. We also provide evidence suggesting metabolic regulation of the priming of granules in the β-cell and finally discuss how defects of β-cell metabolism (8,9) may contribute to the secretory deficiency characterizing type 2 diabetes.

QUANTITATIVE ASPECTS OF BIPHASIC INSULIN SECRETION

It is well established that glucose-stimulated insulin secretion follows a characteristic biphasic time course (Fig. 1*B*) (10). Shortly (1–2 min) after elevation of the glucose concentration, a transient component of insulin secretion is observed. In mouse islets, this component has a duration of <10 min and reaches a peak secretory rate of 50–100 pg of insulin per minute and islet (first phase). The secretory rate then declines and plateaus at a lower secretory rate of 10–80 pg per minute and islet (depending on the experimental conditions), which continues as long as glucose remains elevated (second phase). Only fuel secretagogues are capable of eliciting the second phase, and when insulin release is initiated by nonmetabolizable stimuli, such as high extracellular K^+ and tolbutamide, only first-phase release is observed (11).

From the Department of Molecular and Cellular Physiology, Institute of Physiology, Lund University, Lund, Sweden.

Address correspondence and reprint requests to patrik.rorsman@mphy.lu.se.

Accepted for publication 20 June 2001.

$[Ca^{2+}]_i$, cytoplasmic Ca^{2+}-concentration; DIDS, 4,4-diisothiocyanostilbene–2,2-disulfonate; fF, femtofarad; IRP, immediately releasable pool; NSF, *N*-ethylmaleimide-sensitive fusion; RRP, readily releasable pool of granules; SNAP, soluble NSF-attachment protein; SNARE, SNAP receptor.

The symposium and the publication of this article have been made possible by an unrestricted educational grant from Servier, Paris.

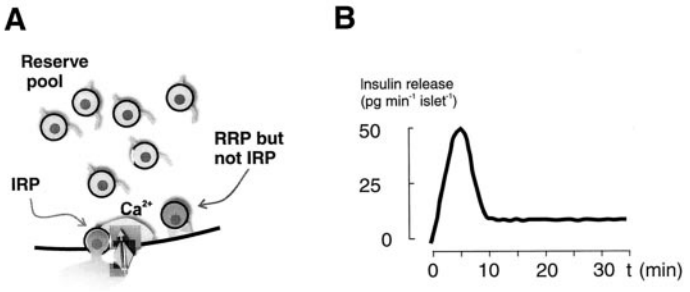

FIG. 1. *A*: Scheme illustrating the existence of distinct granule pools. The granules of belong either to the RRP or a reserve pool. The transition from the reserve pool to RRP involves either physical translocation and/or chemical modification of secretory granules and is referred to as priming. In β-cells, most RRP granules are situated in the immediate vicinity (~10 nm) of the L-type Ca^{2+} channels. These granules are instantly exposed to exocytotic concentrations of Ca^{2+} upon opening of Ca^{2+}-channel activation and are released with minimal latency (IRP). *B*: Scheme of biphasic insulin secretion in response to stimulation with glucose.

The secretory rates quoted above can be converted to number of granules undergoing release, as a single granule contains 2 femtogram insulin (equivalent to ~250,000 molecules of insulin) and assuming that a typical islet contains 1,000 β-cells. As discussed elsewhere (5,12), these calculations suggest that first-phase insulin secretion corresponds to the total release of 50–100 granules per β-cell and that second-phase release amounts to 5–40 granules per cell and minute.

PROBLEMS EQUATING INCREASES IN CELL CAPACITANCE TO INSULIN SECRETION

Before considering our experimental data, a few words about the method we used to measure exocytosis (capacitance measurements) may be appropriate. A confounding feature of capacitance measurements is that they almost invariably indicate rates of exocytosis much higher than expected from reported values of insulin secretion. Accordingly, the 5 granules per minute we derived above as the lower value of glucose-induced second-phase insulin secretion corresponds to 300 granules (2.5% of total granule number) per hour. However, the maximum rate of capacitance increase observed in β-cells is equivalent to 600 granules (5% of total granule number) per second. Thus, there appears to be a discrepancy of almost four orders of magnitude! However, it is important to remember that this high rate of exocytosis detected by capacitance measurements only proceeds for a brief period (<0.5 s) and that exocytosis in the steady state is considerably slower (<15 granules per second). It also deserves pointing out that capacitance measurements only report changes in the cell surface area (equal to membrane fusion). Obviously, there might be significant delays between the fusion of the granules with the plasma membrane, the establishment of the (narrow, ~1 nm) fusion pore and cargo release. Recent observations in our laboratory suggest that there is indeed a significant delay (1–10 s) between membrane fusion and release of insulin (S.B., C.S. Olofsson, J. Schriever-Abeln, A. Wendt, S. Gebre-Medhin, E.R., P.R., submitted). Interestingly, there is evidence that the opening of the fusion pore in eosinophils is modulated by Ca^{2+} and protein kinase C (13). If this also occurs in β-cells, then regulation of insulin secretion at a very distal level (i.e., subsequent to elevation of cytoplasmic Ca^{2+} and membrane fusion) can be envisaged.

ASSOCIATION OF SECRETORY GRANULES TO CA^{2+} CHANNELS

The pancreatic β-cell is an interesting example of Ca^{2+}-induced hormone release because it is capable of a high-speed exocytosis, even though it is equipped with <500 Ca^{2+} channels (estimated by nonstationary fluctuation analysis) (14). The β-cell has a cell capacitance of 5 pF. Using a conversion factor of 10 femtofarad (fF)/μm^2, we can estimate that the cell surface area is ~500 μm^2, indicating a Ca^{2+}-channel density of <1 Ca^{2+} channel/μm^2. This should be compared with the Ca^{2+}-channel density in adrenal chromaffin cells (the archetypal endocrine cell), which has been estimated to range between 9 and 20 Ca^{2+} channels (15,16). Although the Ca^{2+}-channel density of the β-cell is thus only 5–10% of that in the chromaffin cells, the secretory capacity is not correspondingly reduced. The maximum rate of exocytosis measured in mouse β-cells during a voltage-clamp depolarization is 1.2 pF/s, 40% of the 3 pF/s observed in chromaffin cells (17). This also holds true if we compare the Ca^{2+}-channel density and peak exocytotic rate in β-cells with the corresponding values in glucagon-producing α-cells. The Ca^{2+}-current density in α-cells measured during depolarizations from –70 mV to 0 mV at 2.6 mmol/l extracellular Ca^{2+} is 39 ± 4 pA/pF ($n = 9$), threefold higher than the 13 ± 2 pA/pF ($n = 8$; $P < 0.001$) observed in β-cells of the same preparation and using the same experimental protocol (standard whole-cell recordings at +32°C and using pipettes containing [mmol/l] 125 Cs-glutamate, 10 CsCl, 10 NaCl, 1 $MgCl_2$, 5 HEPES, 0.05 EGTA, 3 Mg-ATP, and 0.1 cAMP). Despite this, the maximum rate of exocytosis is only 35% higher in the α-cell (1.7 pF/s) (18) than in the β-cell (1.2 pF/s). Collectively, these findings argue that there exists a tight assembly of Ca^{2+} channels and secretory granules in the β-cell and that the coupling between Ca^{2+} entry and exocytosis is more efficient than in other secretory cells such as glucagon-releasing β-cells and adrenaline-producing chromaffin cells.

What is the mechanism behind the economical use of Ca^{2+} in the β-cell? We have previously proposed that L-type Ca^{2+} channels and secretory granules colocalize in the β-cell (19). More recently, we demonstrated that a peptide of the α_{1C}-subunit of the L-type channel (the only L-type channel in β-cells isolated from Naval Medical Research Institute mice) (14), corresponding to the synprint site ($Lc_{753\text{-}893}$; "synprint"), binds to immobilized syntaxin, SNAP-25, and p65 (20). It has been shown that injecting the corresponding region of N-type Ca^{2+} channels abolishes fast neurotransmission (21). In β-cells, exogenous synprint suppressed exocytosis evoked by single (500 ms) voltage-clamp depolarizations. The latter effect could not be attributed to inhibition of Ca^{2+} entry or interference of exocytosis per se as witnessed by the lack of effect on the peak Ca^{2+} current and exocytosis triggered by a global increase in cytoplasmic Ca^{2+}-concentration ($[Ca^{2+}]_i$) through flash photolysis of "caged" calcium (20). Thus, exocytosis in pancreatic β-cells is more neuron-like than what was perhaps anticipated.

Taken together with biochemical data, it seems likely

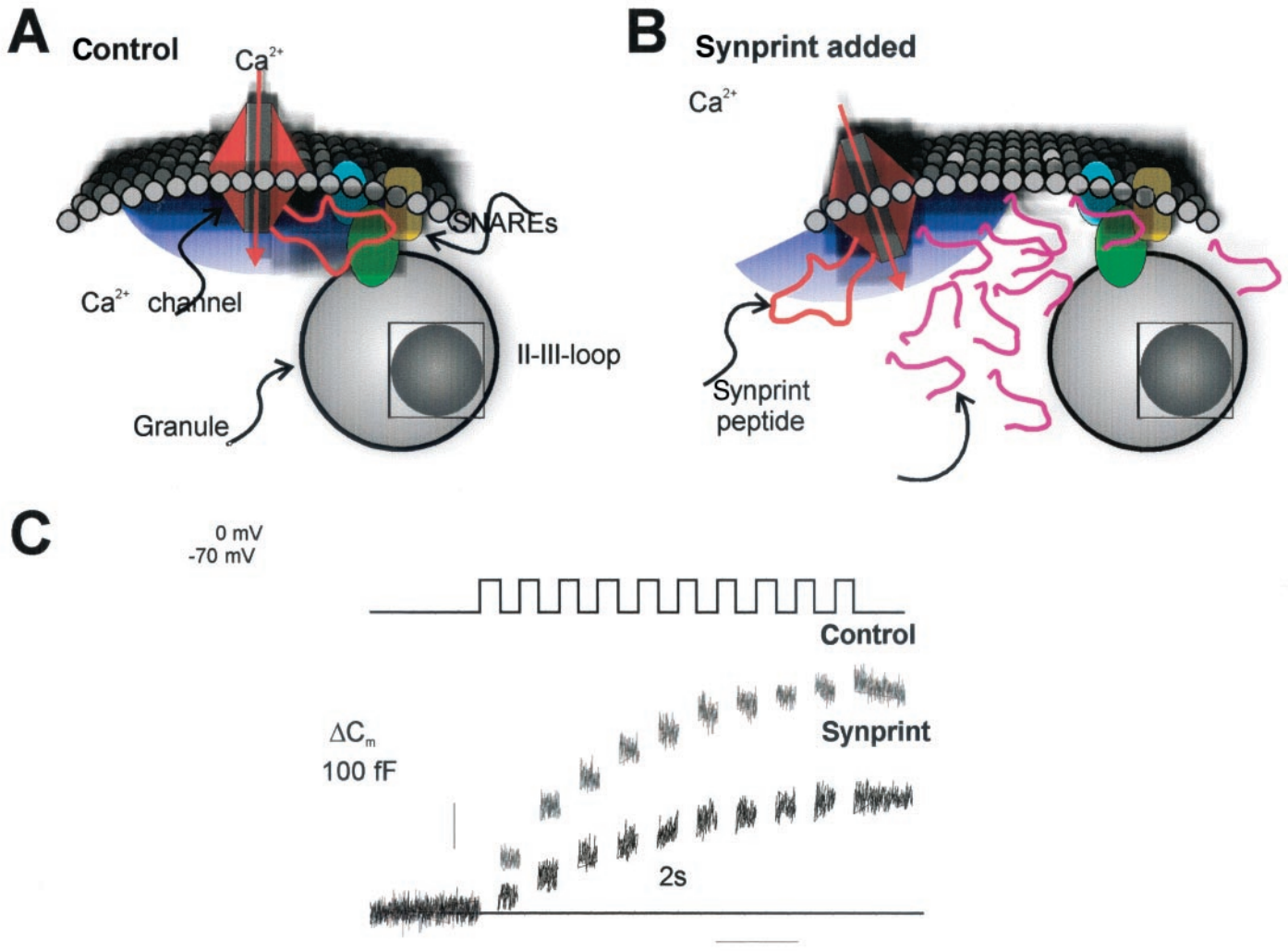

FIG. 2. Exogenous synprint peptide uncouples the Ca^{2+} channel from the exocytotic machinery. *A*: SNAREs bind to the II-III loop of the L-type (α_{1C}) Ca^{2+} channel and thereby tether the granule to the vicinity of the inner mouth of the channel. *B*: Addition of a large excess of the synprint peptide competes with the channel's II-III loop leading to the disassembly of the granule-channel complex. *C*: Typical recordings of capacitance increases in a β-cell in response to a train of ten 500-ms depolarizations from –70 to 0 mV under control conditions and in the presence of 2.5 μmol/l exogenous synprint peptide. Note that the action of the synprint peptide is particularly strong on the response to the first depolarization. Data in *C* are taken from reference 14, where a full description of the experimental conditions can be found.

that the synprint region of the L-type Ca^{2+} channels tethers it to the secretory granules, thus ensuring that the exocytotic machinery is rapidly exposed to very high Ca^{2+} concentrations upon Ca^{2+}-channel opening (Fig. 2*A*). Such a concept would account for both the ability of the β-cell to perform high-speed exocytosis despite the low Ca^{2+}-channel density and the fact that exocytosis in the β-cell normally proceeds only during the depolarization (22). Adding a high concentration of exogenous synprint peptide competes for the binding site on the granule with the endogenous polypeptide loop that is part of the L-type Ca^{2+} channels (Fig. 2*B*). This leads to dissociation of the Ca^{2+} channel–SNARE/synaptotagmin complex, thereby increasing the average distance between channels and docked granules. This interpretation is supported by the finding that, although exocytosis elicited by single depolarizations is abolished by the synprint peptide, it can be rescued by a train of depolarizations applied at a high frequency (Fig. 2*C*). This is presumably a consequence of the interval between two successive depolarizations (500 ms) being too short for $[Ca^{2+}]_i$ to return to basal, leading to a progressive accumulation of Ca^{2+} inside the cell. Eventually, the global Ca^{2+} concentration has risen sufficiently to trigger exocytosis of granules situated too far away from the Ca^{2+} channels to be released by a single stimulation.

MANY RRP GRANULES ARE TETHERED TO THE Ca^{2+} CHANNELS IN β-CELLS.

Analysis of the kinetics of depolarization-evoked exocytosis has revealed a rapid component of capacitance increase (presumably the β-cell equivalent of IRP) with an amplitude of ~100 fF that is released with a time constant of 75 ms and that plateaus within 100–200 ms (Fig. 3*A*). This component is highly sensitive to inclusion of the synprint peptide, suggesting that it reflects the release of granules that have complexed with the Ca^{2+} channels (14). Interestingly, the size of this component is comparable to a rapid component of capacitance increase observed in response to a step elevation of $[Ca^{2+}]_i$ by photorelease of caged Ca^{2+}, which likely corresponds to RRP (Fig. 3*C*)

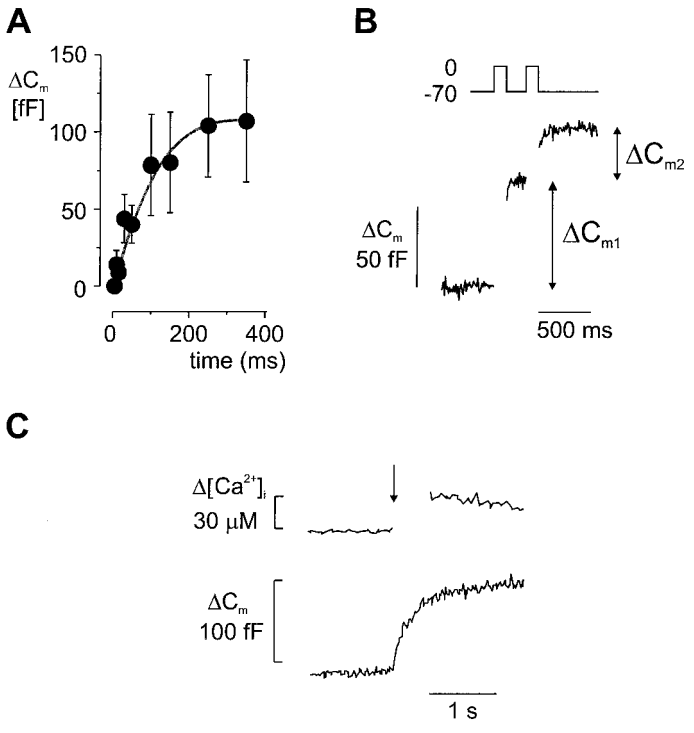

FIG. 3. A fast component of exocytosis corresponding to a capacitance increase of 100 fF revealed by three different methods. *A*: Relationship between pulse length and exocytotic response measured as capacitance increase (ΔC_m). The longer the depolarization, the more Ca^{2+} enters the cell leading to greater exocytotic responses. Note that the capacitance increase saturates for depolarizations >200 ms. (Data from reference 14). *B*: Size of IRP determined using the two-pulse protocol first described by Gillis et al. (23). The assumption is that the cell contains a readily releasable pool of granules, all of which have the same release probability. The first depolarization leads to substantial depletion of this pool. The Ca^{2+} entering the cell during the second depolarization has fewer granules to act on, and the exocytotic response is consequently reduced. The number of granules belonging to IRP (in fF) can then be estimated by the equation IRP = S/(1 − R^2), where S represents the sum of the capacitance responses to the first (ΔC_{m1}) and second (ΔC_{m2}) depolarizations (as indicated), and R is the $\Delta C_{m2}/\Delta C_{m1}$ ratio. This analysis depends on the fact that significant depression occurs during the two pulses, and the amplitude of the response to the second depolarization must be ≤70% of that elicited by the first depolarization. Only these experiments were included. The size of IRP in this cell was estimated to be 101 fF (50 granules). *C*: Capacitance increase evoked by a step increase in $[Ca^{2+}]_i$ of ~30 μmol/l effected by photorelease from caged Ca^{2+} (effected at arrow). Note rapid increase in cell capacitance that plateaus within 0.5 s at ~100 fF. Data in *C* modified from reference (5).

(5). Thus, it appears as if all RRP granules in the β-cells are situated in close proximity of the Ca^{2+} channels and thus identical to the IRP. If there were many more RRP granules than IRP granules, then a rapid global increase in Ca^{2+} would be expected to produce a much larger exocytotic response than that elicited by brief membrane depolarizations. However, estimating pool sizes from experiments using caged Ca^{2+} is complicated by concomitant and rapid endocytosis and the capacitance changes observed represent the net changes, which might result in a too low value of RRP. Indeed, when only including experiments lacking endocytosis, RRP was found to be >200 fF (C. Olofsson, S. Göpel, S.B., J. Galvanovskis, X. Ma, A. Salehi, P.R., L.E., submitted). We also estimated IRP using the two-pulse protocol first described by Gillis et al. (23). The size of IRP was estimated by two 100-ms pulses (i.e., the time where depolarization-evoked exocytosis starts to plateau; cf., Fig. 3*A*) applied with an interval of 200 ms (Fig. 3*B*). We thus derived a size of IRP of 102 ± 18 fF (n = 5), equivalent to 50 granules using a conversion factor of 2 fF/granule (22), similar to the synprint-sensitive component. It therefore seems justifiable to conclude that in mouse β-cells, up to 50% of the release-competent RRP granules are situated in the immediate vicinity of a Ca^{2+} channel (14).

If the IRP granules in the β-cell are all tethered to the Ca^{2+} channels via the synprint region of the Ca^{2+}-channel protein, then the length of the peptide can be used to estimate the maximum distance between the mouth of the Ca^{2+} channel and the Ca^{2+} sensor. The synprint region contains 140 residues. Given that each residue contributes 1.5 Å (as expected, assuming α-helical organization) to the peptide chain, then the total length of the synprint peptide is ~20 nm. From this, we infer that an IRP granule is situated ≤10 nm from a Ca^{2+} channel. This close to the Ca^{2+} channels, the Ca^{2+} concentration can be expected to rise to very high levels (24). Using caged Ca^{2+} to produce uniform and rapid increases in $[Ca^{2+}]_i$, we have estimated the Ca^{2+} dependence of exocytosis in the β-cell. The speed of exocytosis was half maximal at ~20 μmol/l $[Ca^{2+}]_i$, and concentrations >30 μmol/l are required to attain the maximum speed of capacitance increase observed during voltage-clamp depolarizations (1.2 pF/s) (14). This Ca^{2+} dependence of exocytosis is close to that observed in preparations with a much higher Ca^{2+}-channel density, such as the adrenal chromaffin cell (25) and central synapses (26,27). However, in a cell with as few Ca^{2+} channels as the β-cell, such high Ca^{2+} concentrations cannot arise, except in the immediate vicinity of the Ca^{2+} channels. For insulin secretion to occur, it is therefore essential that the release-competent secretory granules are situated close to the points of Ca^{2+} entry.

FUNCTIONAL ADVANTAGES OF TIGHT COUPLING BETWEEN CA^{2+} ENTRY AND EXOCYTOSIS

What is the functional advantage of tethering Ca^{2+} channels to the secretory granules? It seems unlikely that speed is the prime objective because insulin acts systemically following its release into the blood stream. Rather, the arrangement is likely to be a consequence of the low Ca^{2+}-channel density. With so few Ca^{2+} channels, it is naturally important that the Ca^{2+} entering the cell is made use of in the most efficient way. This is achieved if the Ca^{2+} channels and secretory granules assemble into a functional complex. By this arrangement, the β-cell can achieve large exocytotic responses over long periods, while minimizing the Ca^{2+} influx and the subsequent expenditure of metabolic energy to restore the Ca^{2+} concentration to the resting level. Removal of Ca^{2+} from the cytoplasm by ATP-consuming Ca^{2+}-ATPases can be expected to lower the cytoplasmic ATP/ADP ratio. Indeed, such an effect has been observed following depolarization-induced Ca^{2+} entry (28). This is obviously undesirable in a cell that utilizes ATP-regulated K^+ channels to control the membrane potential. Excessive Ca^{2+} entry can then be expected to lower the cytoplasmic ATP/ADP ratio sufficiently to activate the K_{ATP} channels and thus prematurely repolarize the β-cell. Apparently, there is less need for the α-cell to economize with Ca^{2+} entry. The Ca^{2+}-channel density is threefold higher in the β-cells than in the β-cell, but the maximum speed of exocytosis is only 35% greater.

Although we have not yet tested the effects of the synprint peptide in α-cells, it is tempting to speculate that its effects are less pronounced than in the β-cell. Because of the high Ca^{2+}-channel density in the α-cell, many RRP granules may be situated close enough to the Ca^{2+} channels to undergo rapid release following the opening of the channels (i.e., they functionally behave as IRP) and they need not be physically attached to the channel protein. A similar argument has been invoked in chromaffin cells to account for an ultrafast component of depolarization-induced exocytosis in these cells (17). Indeed, less efficient coupling between Ca^{2+} entry and secretion in α-cells and chromaffin cells is not unexpected, given that both adrenaline and glucagon need only be released for brief periods, but at a high rate under certain physiological conditions, such as hypoglycemia and intense labor. By contrast, insulin must be provided, more or less continuously, throughout life.

RELATIONSHIP BETWEEN RRP AND DOCKED POOL

Electron microscopy on various neuronal and endocrine cells (29–31) has revealed a subset of secretory granules that are docked beneath the plasma membrane, but the precise relationship between the docked pool and RRP is not entirely clear. A similar situation appears to exist in the pancreatic β-cell, where the number of ultrastructurally docked granules is ~10-fold larger than the functionally determined size of IRP/RRP (Olofsson C, Göpel S., S.B., J. Galvanouskis, X. Ma, A. Salehi, P.R., L.E., submitted). Therefore, refilling of RRP following its emptying does not necessarily involve the physical translocation of secretory vesicles. Recent experiments using a combination of capacitance measurements and confocal imaging of EGFP-tagged secretory granules (S.B., C.S. Olofsson, J. Schriever-Abeln, A. Wendt, S. Gebre-Medhin, E.R., P.R., submitted) indicate that replenishment of RRP principally reflects priming of granules already docked below the membrane. Given that replenishment of RRP does not correlate with any granule movements and the data suggesting that all RRP granules associate with the Ca^{2+} channels, it appears necessary to postulate a mechanism for disassembly of the Ca^{2+} channel/granule complexes following exocytosis, so that the Ca^{2+} channels are liberated to associate with new granules. If this is the case, then the Ca^{2+} channels must possess the ability to move laterally within the plasma membrane at sufficient speed to account for the recovery of RRP. It should therefore be interesting to study the mobility of fluorescently tagged Ca^{2+} channels in the plasma membrane and how agents that accelerate RRP recovery affect their mobility.

METABOLIC REGULATION OF GRANULE PRIMING FOR RELEASE

As remarked above, the bout of exocytosis that can be released immediately upon elevation of $[Ca^{2+}]_i$ corresponds to only ~0.5% of the total number of granules. The ability of the cell to maintain the exocytotic capacity in the long term depends on the continuous replenishment of RRP by mobilization of granules from a "reserve pool." The latter process involves ATP-, Ca^{2+}-, and temperature-dependent "priming" reactions (3–6).

Clearly, several sequential steps are necessary to render the granule release-competent. Here we will only consider

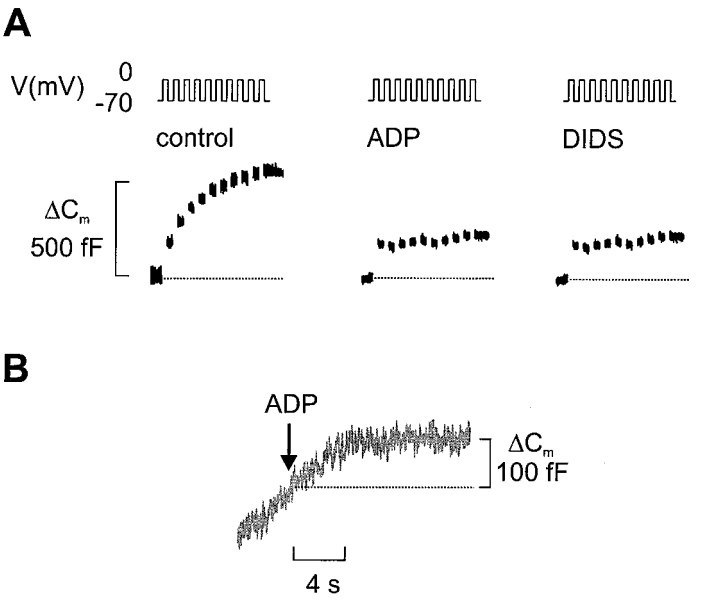

FIG. 4. ADP interferes with the replenishment of RRP. *A*: Exocytosis elicited by a train of 10 voltage-clamp depolarizations under control conditions (3 mmol/l Mg-ATP and 0.1 mmol/l cAMP; left), after supplementing the intracellular medium with 5 mmol/l Mg-ADP (middle) and after inclusion DIDS (0.1 mmol/l) in the pipette-filling solution (right). Note that ADP and DIDS have little effect on the response to the first depolarization, but subsequent depolarizations fail to produce any further increase in cell capacitance. *B*: Gradual increase in cell capacitance elicited by intracellular dialysis with a medium containing 1.5 μmol/l free Ca^{2+} (9 mmol/l Ca^{2+} and 10 mmol/l EGTA), 3 mmol/l Mg-ATP, and 0.1 mmol/l cAMP. At the arrow, 3.5 mmol/l ADP was liberated from a caged precursor. All recordings were obtained in the standard whole-cell configuration. Full experimental details are provided in reference 32.

the possibility that the cell's metabolic state influences granule priming, a feature that may be particularly important in the β-cell that controls fuel homeostasis of the entire body. Figure 4*A* (left) shows the increases in cell capacitance evoked by a train of 10 depolarizations. It can be seen that the total increase amounts to ~500 fF. In a series of nine experiments, the total increase in cell capacitance evoked by the train averaged 363 ± 61 fF, 3.5-fold larger than the size of RRP estimated by the two-pulse protocol (see above). This suggests that RRP must have turned over several times during the pulse train and that granule priming operates at sufficient speed to allow RRP recovery within a few seconds. We subsequently repeated the experiment in the presence of 5 mmol/l Mg-ADP but maintained the concentrations of ATP and cAMP at 3 mmol/l and 0.1 mmol/l, respectively (Fig. 4*A*, middle). Exocytosis under the latter conditions is much reduced and the total increase in cell capacitance elicited by the train was only ~100 fF (100 ± 16 fF in a series of four experiments). However, close inspection revealed some interesting features. Thus, the capacitance increase evoked by the first depolarization was hardly affected and averaged 130 ± 35 fF and 90 ± 11 fF under control conditions and in the presence of ADP, respectively. The latter value is close to the size of IRP/RRP estimated as described above, suggesting that exocytosis of granules that have already proceeded into RRP is unaffected by ADP. The inhibitory action of ADP is instead exerted at the level of granule priming and replenishment of RRP, manifested as the loss of the progressive capaci-

tance increase normally observed in response to depolarization numbers 2–10.

We also tested the effects of rapid application of ADP (3.5 mmol/l) by release from a caged precursor. Figure 4*B* shows an experiment in which exocytosis was elicited by intracellular dialysis with a medium containing 3 mmol/l Mg-ATP, 0.1 mmol/l cAMP, and 1.5 μmol/l $[Ca^{2+}]_i$ (mixture of 9 mmol/l Ca^{2+} and 10 mmol/l EGTA, pH 7.15). The rate of capacitance increase under control conditions averaged 30 ± 5 fF/s. Application of ADP reduced the rate of exocytosis to 3 ± 4 fF/s ($n = 6$; $P < 0.01$ vs. control). However, the inhibitory effect of ADP was not instantaneous, but occurred with a latency of 4 ± 1 s. During this period, the cell capacitance increased by 98 ± 10 fF. The latter value is again close to that which remained releasable during the train of depolarizations in the presence of ADP and the size of RRP estimate by the two-pulse protocol.

MOLECULAR MECHANISMS INVOLVED IN PRIMING

How does the metabolic state, as evidenced by the effects of changing the ATP/ADP ratio, regulate exocytosis? Experiments using Cl^- channel blockers, such as 4,4-diisothiocyanostilbene–2,2-disulfonate (DIDS), as well as omission of intracellular Cl^-, implicate granular Cl^- fluxes in the regulation of exocytosis (32). Indeed, two antibodies against the Cl^- channel ClC-3 labeled β-cell granules. The antibody anti–ClC-3-C, which has been demonstrated to block ClC-3 channel function, abolished exocytosis in β-cells when included in the intracellular solution (32). This was neither due to unspecific interaction nor steric hindrance of the exocytotic machinery, because the antibody anti–ClC-3-N, which lacks effect on ClC-3 channel activity, was without inhibitory action on exocytosis. It is therefore not unexpected that intracellular application of DIDS (0.1 mmol/l) abolishes exocytosis elicited by a train except for the response to the first depolarization (Fig. 4*A*, right). The effects of the Cl^- channel blocker clearly resemble those of ADP (cf. Figure 4*A*, middle), suggesting that granular Cl^- uptake is somehow required in the preparation of granules for release.

What is the significance of granular Cl^- uptake? We can discard the possibility that net accumulation of electrolytes and associated water uptake promotes exocytosis via increased intragranular hydrostatic pressure (33–35) because varying the osmolarity of the cytosol over a wide range (300–1,000 mOsm) did not influence exocytosis (32). Alternatively, the electrogenic H^+ pumping, involved in the acidification of the granule interior, might require a shunt conductance to prevent the development of a large electrical potential across the granular membrane (36). Indeed, both inhibition of the granular v-type H^+-ATPase with bafilomycin and disruption of the granular pH gradient using the protonophore CCCP (carbonyl cyanide *m*-chlorophenylhydrazone) resulted in strong suppression of Ca^{2+}-induced exocytosis (32). This implicates granular acidification as an important step in the priming of the secretory granules. We verified this concept by correlating exocytosis to changes in intragranular pH. In these experiments, intragranular pH was measured with the fluorescent probe LysoSensor green, which accumulates in acidic compartments (mostly granules in the β-cell) and that is virtually nonfluorescent at neutral pH. Figure 5*A* shows changes in cell capacitance evoked by intracellular dialysis with a solution containing 1.5 μmol/l Ca^{2+}, 3 mmol/l Mg-ATP, and 0.1 mmol/l cAMP. It can be seen that cell capacitance increases by >2 pF over 60 s, and the average rate of capacitance increase was 32 ± 5 fF/s ($n = 26$). Including 5 mmol/l ADP in the intracellular solution resulted in strong inhibition of exocytosis, and the rate of capacitance increase averaged 8 ± 3 fF/s ($n = 12$; $P < 0.01$ vs. control [no ADP]). The effects of ADP were virtually identical to those of DIDS, and the mean rate of capacitance increase in the presence of the Cl^--channel blocker was 8 ± 4 fF/s ($n = 8$; $P < 0.01$). Figure 5*B* correlates the exocytotic responses to changes of intragranular pH in cells that had been preloaded with LysoSensor. It can be seen that the granules acidify promptly following establishment of the whole-cell configuration and wash-in of the high ATP-solution. This acidification could be prevented by inclusion of ADP. Again, the effects of ADP on granule pH were mimicked by DIDS.

Figure 5*C* attempts to summarize the chain of events that are involved in granule priming. We propose that granular acidification is a decisive event and depends on the simultaneous activity of the v-type H^+-ATPase and the ClC-3 Cl^- channel. Granular Cl^- uptake counteracts the development of an insurmountable electric field across the membrane (positive inside), which would prevent further H^+ pumping and intragranular acidificaiton. In this scenario, Ca^{2+} and ATP enhance granular Cl^- uptake and thus facilitate H^+ pumping and granule priming, whereas ADP, by inhibiting ClC-3 (compare with the effects of DIDS), prevents granular acidification and priming. There are similarities between this concept and the recently postulated role of granular glutamate uptake in insulin secretion from rat β-cells (37). In both cases, the uptake of the anion by allowing granule acidification increases granule releasability.

This mechanism may not be limited to pancreatic β-cells, as Cl^- is required for hormone release in a variety of other cells, including pancreatic acinar cells (38) and pituitary melanotrophs (39). Very recent data also suggest that ClC-3 channels fulfill an important function in the acidification of synaptic vesicles (40). What is the role of granular acidification in granule priming? Possibly, low granular pH promotes exocytosis by inducing conformational changes in SNARE proteins, rendering them more fusogenic (41).

A GENERAL MODEL FOR BIPHASIC INSULIN SECRETION

Based on the findings reviewed above, we propose the following model to account for biphasic insulin secretion (Fig. 6). We believe that first-phase insulin secretion is attributable to the release of RRP granules. A host of experimental data suggests that this pool is limited to 50 granules (giving rise to a capacitance increase of 100 fF upon fusion) in mouse pancreatic β-cells (Fig. 6*A*). A remarkable feature of the β-cell is that nearly all RRP granules are situated in close proximity to the few (<500 per cell) Ca^{2+} channels and undergo exocytosis within 100–200 ms (Fig. 6*B*). The size of RRP granules compares

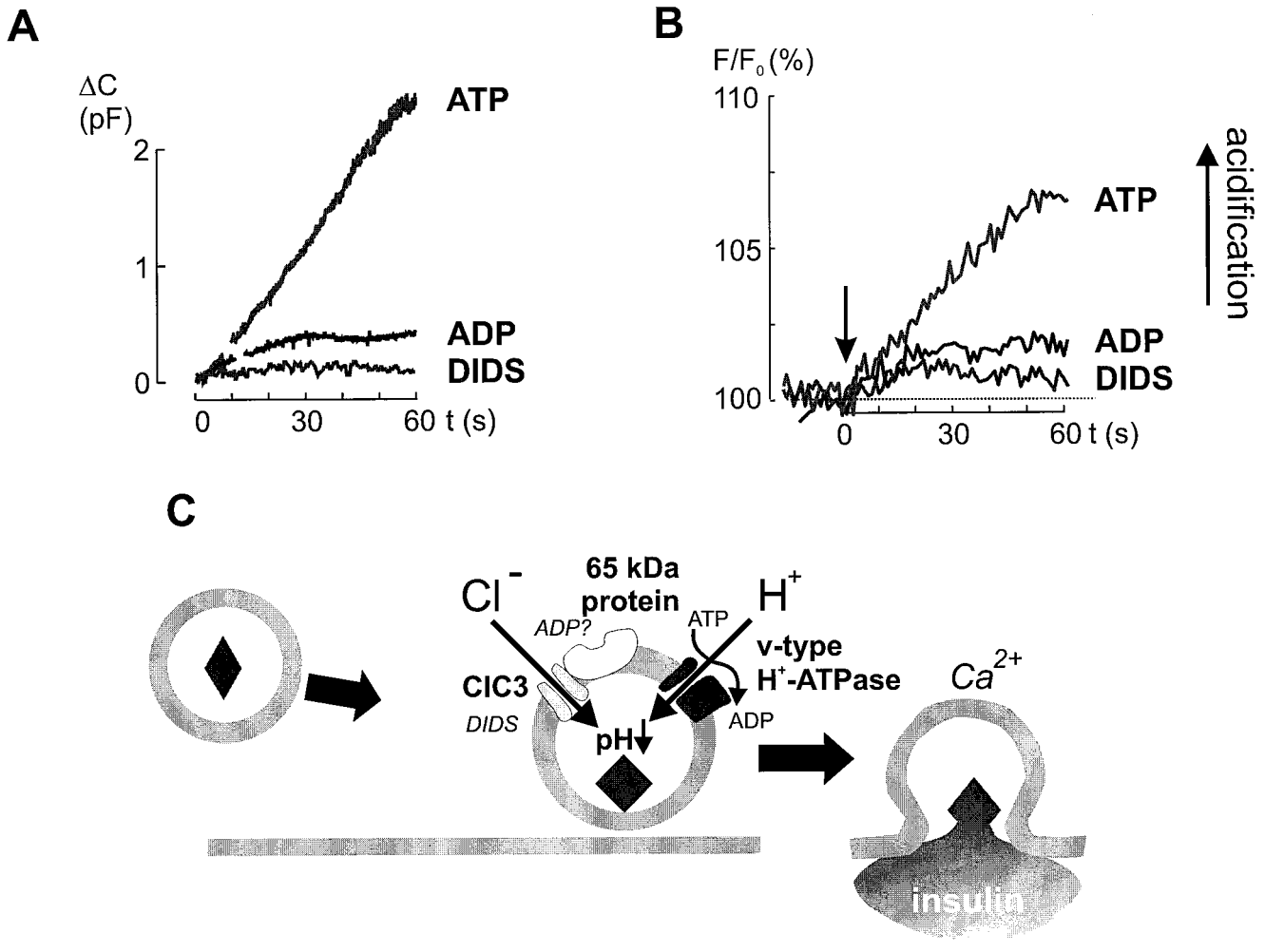

FIG. 5. Granule priming involves granular acidification. *A*: Increases in cell capacitance (ΔC) under control conditions and after addition of 5 mmol/l Mg-ADP or 0.1 mmol/l DIDS. Secretion was elicited by intracellular dialysis with a medium containing 1.5 μmol/l free Ca^{2+} (9 mmol/l Ca^{2+} and 10 mmol/l EGTA), 3 mmol/l Mg-ATP, and 0.1 mmol/l cAMP. *B*: Changes in granular pH measured using LysoSensor under control conditions and after supplementing the intracellular medium with 5 mmol/l Mg-ADP or 0.1 mmol/l DIDS. The whole-cell configuration was established at the time indicated by the left arrow. An upward deflection corresponds to granular acidification (right arrow). Note that ADP prevents acidification resulting from dialysis with the ATP solution. Data in *A* and *B* are taken from reference 32. *C*: Metabolic regulation of granule priming. Cl^- uptake through an ion channel complex comprised of DIDS-sensitive ClC-3 Cl^- channels and an mdr1-like 65 kDa protein (37) determines the extent of granular acidification by providing the counterion required to allow continuous H^+ pumping by a V-type H^+-ATPase. Once granular acidification has occurred, granules can undergo exocytosis whenever $[Ca^{2+}]_i$ increases to exocytotic levels.

favorably with the total number of granules that are released during first-phase insulin secretion (Fig. 6*C*). We further propose that refilling of IRP/RRP by priming of granules accounts for second-phase insulin secretion. Capacitance measurements using intracellular dialysis with high $[Ca^{2+}]_i$ buffers (1.5 μmol/l) to trigger exocytosis have revealed that secretion continues for several minutes at a steady rate of 20–30 fF/s (10–15 granules/s). The total increase in cell capacitance under these conditions amounts to ≤5 pF, which is equivalent to the release of ~2,500 secretory granules. Obviously, the 50 granules originally residing in RRP can only account for a few percent of this response, and we therefore conclude that most of the capacitance increase observed under these experimental conditions is due to release of granules mobilized from the reserve pool. The rate of granule mobilization suggested by the capacitance measurements described above (10–15 granules/s) is >10-fold higher than that required to account for second-phase insulin secretion (0.1–0.7 granules/s). Thus, factors other than the supply rate of granules set an upper limit to second-phase insulin secretion. The same conclusion was also reached by Daniel et al. (42) using different methods.

As discussed above, the secretory granules gain release competence subsequent to their intragranular acidification. The observations that ADP prevents granular acidification, granule priming, and refilling of RRP may explain why stimulation with tolbutamide or high extracellular K^+ only produces a transient stimulation of insulin release when they are applied in the absence of glucose. This is because only granules that have proceeded into RRP are capable of undergoing exocytosis under these experimental conditions, and the replenishment of this pool is largely prevented by the high cytoplasmic ADP concentration.

Type 2 diabetes is associated with metabolic disturbances interfering with the generation of ATP (8,9). The finding that ADP prevents the refilling of RRP may thus also account for the low insulin secretory capacity associated with the disease. It is therefore of interest that sulfonylureas such as tolbutamide, in addition to closing

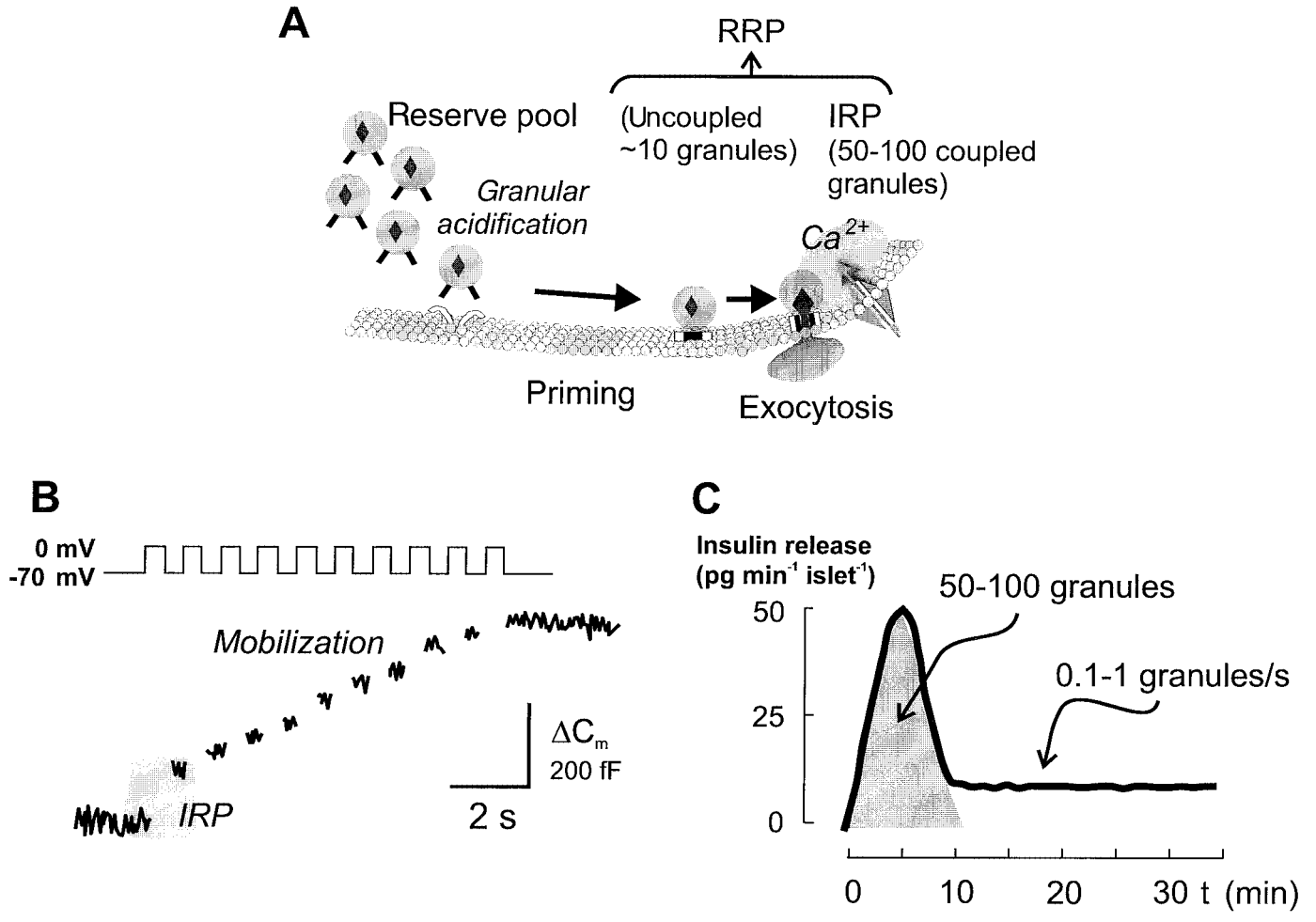

FIG. 6. Model for biphasic insulin secretion in the β-cell. *A*: Rapid release of the RRP underlies first-phase insulin secretion. RRP comprises only 50 granules in the β-cell, of which nearly all are situated in the immediate vicinity of the Ca^{2+} channels IRP. Replenishment of RRP/IRP by priming granules originally belonging to the reserve pool depends on intracellular acidification. *B*: Components of capacitance increase and the contribution of the different granule pools. The recording shows the capacitance increases elicited by a train of ten 500-ms depolarizations from –70 to 0 mV applied at 1 Hz. Note that the first depolarization evokes a capacitance increase of ~130 fF and that the capacitance then increases by 40 fF per pulse during the remainder of the train. Of the capacitance increase elicited by the first pulse, 70% is attributable to the release of IRP. We attribute the increase in cell capacitance during the following pulses to mobilization of granules initially in the reserve pool. *C*: Granule pools and biphasic insulin secretion. A total of 50–100 granules are released during first-phase insulin secretion. Second-phase insulin secretion (0.1–0.7 granules per second and cell) requires mobilization and priming of granules that originally belong to the reserve pool.

K_{ATP} channels, also counteract the ability of ADP to inhibit exocytosis (32), an effect that must involve processes other than K_{ATP} channel closure.

ACKNOWLEDGMENTS

Financial support was obtained from the Swedish Medical Research Council (Grants 8647, 9890, 12334, 12708, and 13147), the Swedish Diabetes Association, the Royal Physiographic Society, the Juvenile Diabetes Foundation International, the Knut and Alice Wallenbergs Stiftelse, the Swedish Society for Medical Research, the Crafoord Foundation, the European Community, and the Novo Nordisk Foundation.

We thank our colleagues in Lund for sharing unpublished data.

REFERENCES

1. Neher E, Zucker RS: Multiple calcium-dependent processes related to secretion in bovine chromaffin cells. *Neuron* 10:21–30, 1993
2. Heinemann C, von Rüden L, Chow RH, Neher E: A two-step model of secretion control in neuroendocrine cells. *Pflügers Arch* 424:105–112, 1993
3. Parsons TD, Coorssen JR, Horstmann H, Almers W: Docked granules, the exocytic burst, and the need for ATP hydrolysis in endocrine cells. *Neuron* 15:1085–1096, 1995
4. Renström E, Eliasson L, Bokvist K, Rorsman P: Cooling inhibits exocytosis in single mouse pancreatic B-cells by suppression of granule mobilization. *J Physiol* 494:41–52, 1996
5. Eliasson L, Renström E, Ding WG, Proks P, Rorsman P: Rapid ATP-dependent priming of secretory granules precedes Ca^{2+}-induced exocytosis in mouse pancreatic B-cells. *J Physiol* 503:399–412, 1997
6. Gromada J, Høy M, Renström E, Bokvist K, Eliasson L, Göpel S, Rorsman P: CaM kinase II-dependent mobilization of secretory granules underlies acetylcholine-induced stimulation of exocytosis in mouse pancreatic B-cells. *J Physiol* 518:745–759, 1999
7. Lang J: Molecular mechanisms and regulation of insulin exocytosis as a paradigm of endocrine secretion. *Eur J Biochem* 259:3–17, 1999
8. Efendic S, Wajngot A, Vranic M: Increased activity of the glucose cycle in the liver: early characteristic of type 2 diabetes. *Proc Natl Acad Sci U S A* 82:2965–2969, 1985
9. Wang H, Maechler P, Hagenfeldt KA, Wollheim CB: Dominant-negative suppression of HNF-1α function results in defective insulin gene transcription and impaired metabolism-secretion coupling in a pancreatic β-cell line. *EMBO J* 17:6701–6713, 1998
10. Curry DL, Bennett LL, Grodsky GM: Dynamics of insulin secretion by the perfused rat pancreas. *Endocrinology* 83:572–584, 1968
11. Gembal M, Gilon P, Henquin JC: Evidence that glucose can control insulin

release independently from its action on ATP-sensitive K^+ channels in mouse B cells. *J Clin Invest* 89:1288–1295, 1992
12. Rorsman P, Eliasson L, Renström E, Gromada J, Barg S, Göpel S: The cell physiology of biphasic insulin secretion. *News Physiol Sci* 15:72–77, 2000
13. Scepek S, Coorssen JR, Lindau M: Fusion pore expansion in horse eosinophils is modulated by Ca^{2+} and protein kinase C via distinct mechanisms. *EMBO J* 17:4340–4345, 1998
14. Barg S, Eliasson L, Galvanovskis J, Göpel SO, Obermüller S, Platzer J, Renström E, Trus M, Atlas D, Striessnig J, Rorsman P: Fast exocytosis with few Ca^{2+}-channels in insulin-secreting mouse pancreatic B-cells. *Biophys J*. In press
15. Fenwick EM, Marty A, Neher E: Sodium and calcium channels in bovine chromaffin cells. *J Physiol* 331:599–635, 1982
16. Klingauf J, Neher E: Modeling buffered Ca^{2+} diffusion near the membrane: implications for secretion in neuroendocrine cells. *Biophys J* 72:674–690, 1997
17. Voets T, Neher E, Moser T: Mechanisms underlying phasic and sustained secretion in chromaffin cells from mouse adrenal slices. *Neuron* 23:607–615, 1999
18. Barg S, Galvanovskis J, Göpel SO, Rorsman P, Eliasson L: Tight coupling between electrical activity and exocytosis in mouse glucagon-secreting α-cells. *Diabetes* 49:1500–1510, 2000
19. Bokvist K, Eliasson L, Ämmälä C, Renström E, Rorsman P: Co-localization of L-type Ca^{2+} channels and insulin-containing secretory granules and its significance for the initiation of exocytosis in mouse pancreatic B-cells. *EMBO J* 14:50–57, 1995
20. Wiser O, Bennett MK, Atlas D: Functional interaction of syntaxin and SNAP-25 with voltage-sensitive L- and N-type Ca^{2+} channels. *EMBO J* 15:4100–4110, 1996
21. Mochida S, Sheng ZH, Baker C, Kobayashi H, Catterall WA: Inhibition of neurotransmission by peptides containing the synaptic protein interaction site of N-type Ca^{2+} channels. *Neuron* 17:781–788, 1996
22. Ämmälä C, Eliasson L, Bokvist K, Larsson O, Ashcroft FM, Rorsman P: Exocytosis elicited by action potentials and voltage-clamp calcium currents in individual mouse pancreatic B-cells. *J Physiol* 472:665–688, 1993
23. Gillis KD, Mossner R, Neher E: Protein kinase C enhances exocytosis from chromaffin cells by increasing the size of the readily releasable pool of secretory granules. *Neuron* 16:1209–1220, 1996
24. Neher E: Vesicle pools and Ca^{2+} microdomains: new tools for understanding their roles in neurotransmitter release. *Neuron* 20:389–399, 1998
25. Augustine GJ, Neher E: Calcium requirements for secretion in bovine chromaffin cells. *J Physiol* 450:247–271, 1992
26. Schneggenburger R, Neher E: Intracellular calcium dependence of transmitter release rates at a fast central synapse. *Nature* 406:889–893, 2000
27. Bollmann JH, Sakmann B, Borst JG: Calcium sensitivity of glutamate release in a calyx-type terminal. *Science* 289:953–957, 2000
28. Detimary P, Gilon P, Henquin JC: Interplay between cytoplasmic Ca^{2+} and the ATP/ADP ratio: a feedback control mechanism in mouse pancreatic islets. *Biochem J* 333:269–274, 1998
29. von Gersdorff H, Vardi E, Matthews G, Sterling P: Evidence that vesicles on the synaptic ribbon of retinal bipolar neurons can be rapidly released. *Neuron* 16:1221–1227, 1996
30. Plattner H, Artalejo AR, Neher E: Ultrastructural organization of bovine chromaffin cell cortex-analysis by cryofixation and morphometry of aspects pertinent to exocytosis. *J Cell Biol* 139:1709–1717, 1997
31. Steyer JA, Horstmann H, Almers W: Transport, docking and exocytosis of single secretory granules in live chromaffin cells. *Nature* 388:474–478, 1997
32. Barg S, Huang P, Eliasson L, Nelson DJ, Obermüller S, Rorsman P, Thevenod F, Renström E: Priming of insulin granules for exocytosis by granular chloride uptake and acidification. *J Cell Sci* 114:2145–2154, 2001
33. Zimmerberg J, Whitaker M: Irreversible swelling of secretory granules during exocytosis caused by calcium. *Nature* 315:581–584, 1985
34. Day RN, Hinkle PM: Osmotic regulation of prolactin secretion: possible role of chloride. *J Biol Chem* 263:15915–15921, 1988
35. Woodbury DJ: Evaluation of the evidence for ion channels in synaptic vesicles. *Mol Membr Biol* 12:165–171, 1995
36. al Awqati Q, Barasch J, Landry D: Chloride channels of intracellular organelles and their potential role in cystic fibrosis. *J Exp Biol* 172:245–266, 1992
37. Maechler P, Wollheim CB: Mitochondrial glutamate acts as a messenger in glucose-induced insulin exocytosis. *Nature* 402:685–689, 1999
38. Fuller CM, Deetjen HH, Piiper A, Schulz I: Secretagogue and second messenger-activated Cl^- permeabilities in isolated pancreatic zymogen granules. *Pflügers Arch* 415:29–36, 1989
39. Rupnik M, Zorec R: Cytosolic chloride ions stimulate Ca^{2+}-induced exocytosis in melanotrophs. *FEBS Lett* 303:221–223, 1992
40. Stobrawa SM, Breiderhoff T, Takamori S, Engel D, Schweizer M, Zdebik AA, Bosl MR, Ruether K, Jahn H, Draguhn A, Jahn R, Jentsch TJ: Disruption of ClC-3, a chloride channel expressed on synaptic vesicles, leads to a loss of the hippocampus. *Neuron* 29:185–196, 2001
41. Sutton RB, Fasshauer D, Jahn R, Brünger AT: Crystal structure of a SNARE complex involved in synaptic exocytosis at 2.4 Å resolution. *Nature* 395:347–353, 1998
42. Daniel S, Noda M, Straub SG, Sharp GW: Identification of the docked granule pool responsible for the first phase of glucose-stimulated insulin secretion. *Diabetes* 48:1686–1690, 1999